Radiation Physics and Chemistry 90 (2013) 21–25

Contents lists available at SciVerse ScienceDirect

Radiation Physics and Chemistry

journal homepage: www.elsevier.com/locate/radphyschem

Weisskopf–Ewing and Hauser–Feshbach calculations of photonuclear cross sections used for electromagnetic dissociation

Anne M. Adamczyk [a,*], John W. Norbury [b], Lawrence W. Townsend [a]

[a] University of Tennessee, 315 Pasqua Engineering Building, Knoxville, TN 37996-2300, USA
[b] NASA Langley Research Center, MS 188E, 2 West Reid Street, Hampton, VA 23681-2199, USA

AUTHOR-HIGHLIGHTS

- The Weisskopf–Ewing (WE) theory is reviewed.
- Photonuclear cross sections calculated with WE theory are compared to HF predictions.
- The WE theory and the HF method give similar photonuclear cross sections.
- Qualitative confidence of WE theory for EMD cross section calculations is found.

ARTICLE INFO

Article history:
Received 31 July 2012
Accepted 22 April 2013
Available online 6 May 2013

Keywords:
Photonuclear reactions
Weisskopf–Ewing
Hauser–Feshbach

ABSTRACT

The Weisskopf–Ewing (WE) and Hauser–Feshbach (HF) theory are statistical methods, which are often used to calculate photonuclear cross sections for compound nucleus reactions. In our past work, WE methodology was presented and photonuclear reaction cross sections for nucleon emission were calculated using WE theory. Here, our previous results, which neglect pre-equilibrium emissions and do not include multiple particle emission, are compared to those calculated with HF theory and experimental data. For the reactions considered herein, it is found that the WE theory and HF method are in reasonable agreement below the two neutron separation energy assuming an energy dependent branching ratio for intermediate and heavy nuclei. In addition, qualitative confidence of WE theory for electromagnetic dissociation (EMD) cross section calculations was found.

1. Introduction

Electromagnetic dissociation (EMD) calculations often use Weizsacker–Williams theory (Bertulani and Baur, 1988; Jackson, 1999) and require photonuclear cross sections as input (Norbury and Maung, 2007), as demonstrated by Adamczyk and Norbury (2011). In Adamczyk and Norbury (2011), it was reported that a large part of the uncertainty in the EMD cross section calculation is due to uncertainties in the theoretical treatment of the photonuclear cross section. Adamczyk and Norbury (2011) investigated the replacement of the energy independent branching ratio formalism employed in the nuclear fragmentation model NUCFRG2 (Wilson et al., 1994, 1995) with the Weisskopf–Ewing (WE) theory for photonuclear cross section calculations. Results showed that the WE theory provides photonuclear cross sections that are comparable to those obtained with energy independent branching ratios. However, for most cases, the photonuclear cross sections calculated with WE theory displayed better agreement to experimental cross section data. In addition, employing the WE theory expanded the capability of NUCFRG2 to calculate EMD cross sections for single deuteron, triton, helion, and alpha particle emission. To ensure confidence in the utilization of the WE evaluation method in our previous work, comparisons will be made to photonuclear cross sections calculated with the Hauser Feshbach (HF) method. Both the WE and HF methods will be validated up to the two neutron separation energy against the experimental data of single neutron emission on intermediate and heavy nuclei.

2. Photonuclear cross sections

This paper focuses on photonuclear reactions where a photon interacts with a nucleus, typically at an energy above a few MeV. When a nuclear excitation occurs, the main contribution comes from the giant dipole resonance (GDR); the reaction results in the emission of neutrons, charged particles, or gamma rays.

* Corresponding author. Tel.: +1781 981 2291.
E-mail addresses: aadamczy@utk.edu (A.M. Adamczyk), John.W.Norbury@nasa.gov (J.W. Norbury), ltownsen@utk.edu (L.W. Townsend).

0969-806X/$ - see front matter © 2013 Elsevier Ltd. All rights reserved.
http://dx.doi.org/10.1016/j.radphyschem.2013.04.027

The dominant feature of the cross section for this type of photonuclear reaction is the excitation of the GDR. This excitation gives the photonuclear cross section its typical Lorentzian shape. Exceptions will occur for deformed nuclei, where the cross section is seen as the sum of two Lorentzians and for light nuclei, which often exhibit complicated shapes (Brink, 2008). For light nuclei, the photonuclear cross section will exhibit a broad peak at approximately 24 MeV, while for heavy nuclei, the peak is at about 12 MeV (Hussein, 2003).

The photoparticle total cross section for emitting particle b is given by (Adamczyk and Norbury, 2011; Frobrich and Lipperheide, 1996; Norbury and Townsend, 1986)

$$\sigma(E_\gamma, b) = g_b(E_\gamma)\sigma_{\text{abs}}(E_\gamma), \tag{1}$$

where $g_b(E_\gamma)$ is the branching ratio or probability of a specific decay mode and $\sigma_{\text{abs}}(E_\gamma)$ is the photonuclear absorption cross section. All of the calculated results for $\sigma(E_\gamma, b)$ presented herein use experimental absorption cross section data from IAEA (2000).

3. Statistical methods

The compilation of an all-encompassing photonuclear database is difficult since every isotope of an element must be individually evaluated. The shape and magnitude of a photonuclear cross section vary with the atomic and mass numbers. The unavailability of experimental data for every isotope necessitates the application of nuclear models. The WE and HF theories are statistical methods, which were developed to model compound nucleus reactions. While WE theory provides a relatively simple way of calculating compound nucleus reactions going to continuum states, angular momentum is not conserved. To resolve this issue, Hauser and Feshbach introduced a model that included angular momentum conservation.

3.1. Hauser–Feshbach theory

The HF method (Brink, 1990; Gadioli and Hodgson, 1992; Hodgson, 1987) is a quantum mechanical formalism that accounts for different parity and angular momentum states. It can be used to calculate cross sections for reactions proceeding to continuum and discrete final states. Due to the increase in the number of allowable dynamical paths, the HF method has greater complexity than the WE theory. The more sophisticated HF method is generally favored for calculations of reactions proceeding through a compound nucleus state.

The HF predictions utilized in this paper are found in the IAEA Handbook on photonuclear data for applications—cross sections and spectra (IAEA, 2000), and are from three photonuclear data libraries: The Los Alamos Photonuclear Library, which is evaluated by Los Alamos National Laboratory (LANL); the Korea Atomic Energy Research Institute (KAERI) Photonuclear Library, and the Beijing Photonuclear Library, which is evaluated by the China Nuclear Data Center (CNDC). LANL uses the HF statistical reaction code GNASH (Young et al., 1996) to calculate emission from a compound nucleus. KAERI also utilizes GNASH, in addition to another HF reaction code GUNF (Lui and Zhang, 1998). The GUNF code, which was developed at CNDC, is currently being used by the Beijing Photonuclear Library.

Calculations performed with the HF approach are sensitive to the choice of nuclear level densities and transmission coefficients. In GNASH and GUNF, nuclear level densities are modeled using the Ignatyuk–Gilbert–Cameron formula (Lui and Zhang, 1998; Talou et al., 2006), which is the same approach that was used for the WE results, and will be discussed in detail in Section 3.2.2. The transmission coefficients for particle emissions, in GNASH and GUNF, are determined by optical model potentials (Lui and Zhang, 1998; Talou et al., 2006).

3.2. Weisskopf–Ewing theory

Most nuclear reaction modeling codes utilize the HF method for evaluation of compound nuclear cross sections; however, ALICE-F (Fukahori, 1991) is one code which calculates compound nucleus decay using the WE model. ALICE-F is used by the Japan Atomic Energy Research Institute (JAERI) for the calculation of photonuclear data for the Japan Evaluated Nuclear Data Library (JENDL). Results from JENDL will be used for photonuclear cross section comparisons.

Adamczyk and Norbury (2011) employed WE theory for the calculation of EMD cross sections. However, this reference did not provide a comprehensive and detail-oriented review of WE methodology. The WE theory provides a simple way of calculating compound nuclear reactions going to continuum states due to its straightforward formulation. The energy dependent branching ratio, which was introduced in Section 2, gives the probability that the compound state will decay by emission of particle b. The energy dependent WE branching ratio, as it will be referred to herein, is given by (Adamczyk and Norbury, 2011; Bertulani and Danielewicz, 2004)

$$g_b(E_C^*) = \frac{\Gamma_b(E_C^*)}{\Gamma_{\text{tot}}(E_C^*)}, \tag{2}$$

where Γ_b is the partial decay width for emitting particle b and E_C^* is the excitation energy of the compound nucleus C. For a photonuclear reaction of an intermediate and heavy nuclei within the GDR, the pre-equilibrium emissions play a small role and the excitation energy, E_C^*, is approximately equal to the photon energy, E_γ. Future work will consider using the Monte Carlo intranuclear cascade model (MCMC), which includes multiple nucleon emissions from pre-equilibrium and compound nucleus decay within the GDR energy range.

In the denominator of Eq. (2) is Γ_{tot}, the total width of the compound state, which is given as the sum of the partial widths for proton (p), neutron (n), deuteron (d), triton (t), helion (h≡^{3}He), and alpha (α) emission. Other decay modes are assumed negligible.

According to WE theory, the partial width of the decay in the numerator of Eq. (2) is expressed as

$$\Gamma_b(E_C^*) = \frac{1}{\rho_C(E_C^*)}\frac{M_b(2s_b+1)}{\pi^2\hbar^2}\int_{V_b}^{E_C^*-\epsilon_b}\sigma_{\text{inv}}(E_b)\rho_B(E_C^*-\epsilon_b-E_b)E_b\,dE_b, \tag{3}$$

where M_b, s_b, V_b, ϵ_b, and E_b are the mass, spin, Coulomb barrier, binding energy, and kinetic energy for the emitted particle b, respectively. Also contained in Eq. (3) is the inverse cross section, σ_{inv}, and the nuclear level densities, ρ_C and ρ_B, for the compound nucleus C and the residual nucleus B, respectively. The inverse cross section and the nuclear level densities are input parameters, whose values sensitively impact the partial width of decay formula. The accuracy of these values will determine the reliability of the WE theory. These terms are discussed below.

3.2.1. Inverse cross section

The inverse cross section is the cross section for the formation of the compound nucleus C by the inverse reaction. For charged particles, the Coulomb field has a strong influence on the inverse cross section. The charged particles are repelled and deflected by the Coulomb field, therefore, charged particles must penetrate the Coulomb potential barrier, V. The barrier effect is represented by multiplying the geometric cross section, σ_{geo}, by the Coulomb barrier transmission probability. The charged particle inverse cross

section is expressed as (Gadioli and Hodgson, 1992)

$$\sigma_{\mathrm{inv},c}(E_c)=\begin{cases}\sigma_{\mathrm{geo}}\left(1-\dfrac{V_c}{E_c}\right) & \text{for } E_c>V_c,\\ 0 & \text{for } E_c<V_c,\end{cases} \tag{4}$$

where c stands for one of the charged particles (p, d, t, h, α). For energies below the Coulomb barrier, the charged particle inverse cross section is zero, and for sufficiently large energies, the inverse cross section asymptotically approaches the geometric cross section. The geometric cross section is represented by the classical target area

$$\sigma_{\mathrm{geo}}=\pi R_{0,B}^2, \tag{5}$$

where the nuclear surface is assumed to be a sphere with radius $R_{0,B}$ given by

$$R_{0,B}=r_0\mathcal{A}_B^{1/3}, \tag{6}$$

and $\mathcal{A}_B$ is the atomic mass of the residual nucleus, B. The radius parameter, r_0, is taken to be 1.18 fm.

The tunneling of the Coulomb barrier plays an essential role for the description of the cross sections near the proton threshold. Although Eq. (4) takes into account the decrease of the inverse cross section for lower kinetic energies of emitted charged particles it also assumes zero for kinetic energies below the barrier. A more sophisticated approach based on the WKB approximation would provide more reliable results for the cross sections near the proton binding energy and will be considered in future work. A detailed calculation can be found in Rodrigues et al. (2007).

The inverse cross section for neutrons was once thought to be equal to just the geometric cross section, until Dostrovsky et al. (1959) suggested a form that took into account the energy and mass number dependence

$$\sigma_{\mathrm{inv},n}(E_n)=\begin{cases}C_n\sigma_{\mathrm{geo}}\left(1+\dfrac{\beta_n}{E_n}\right) & \text{for } E_n>\beta_n,\\ 0 & \text{for } E_n<\beta_n,\end{cases} \tag{7}$$

where $\beta_n=(2.12\mathcal{A}_B^{-2/3}-0.050)/C_n$ and $C_n=0.76+2.2\mathcal{A}_B^{-1/3}$. From Eq. (7), it can easily be seen that, for large neutron energies, the neutron inverse cross section will tend towards the geometric cross section. Conversely, as the neutron energy becomes smaller, the neutron inverse cross section will become larger.

3.2.2. Nuclear level density

For the WE calculations presented herein the nuclear level density formula utilizes the Gilbert–Cameron approach (Belgya et al., 2006), since this model was used for the HF predictions, given by the GNASH and GUNF nuclear reaction codes. The Gilbert–Cameron approach, which is based on a Fermi-gas model, is popular due to its simplicity; energy levels are equally spaced and non-degenerate. While this model contains little physical information and is quite unrealistic, it is generally used due to its simple formalism and is employed herein to maintain consistency with the HF predictions.

In this work, we opt for a simplified level density which differs from Belgya et al. (2006) by only the omission of a pre-exponential factor. The level density is approximated as

$$\rho(E^*)\approx\exp[2(aE^*)^{1/2}], \tag{8}$$

where a is the level density parameter.

The HF predictions of GNASH and GUNF employ a nuclear level density that includes a multiplicative term, which is a function of excitation energy. There, the level density is expressed as (Belgya et al., 2006)

$$\rho(E^*)=\frac{\sqrt{\pi}}{12a^{1/4}E^{*5/4}}\exp[2(aE^*)^{1/2}]. \tag{9}$$

Above 1 MeV, the effect of the excitation energy dependent multiplicative term is negligible due to the dominant nature of the exponential function. All of the photonuclear results have a minimum energy above 1 MeV, so the approximated nuclear level density formula, Eq. (8), can be used to allow for faster computations without loss of information.

The level density parameter is often considered as an adjustable parameter that is determined by comparison to experiment (Dostrovsky et al., 1958). In this work, an energy dependent expression is used for the level density parameter, which introduces more complexity into the partial width equation (3), but reproduces experimental level density parameters quite well. Note that the level density parameter employed for the WE calculations presented herein is the same parameter used for the HF predictions given by the GNASH and GUNF nuclear reaction codes.

The level density parameter is defined by (Ignatyuk et al., 1975)

$$a(E^*)=\tilde{a}\left[1+\frac{\delta E_0}{E^*}[1-\exp(-\gamma E^*)]\right], \tag{10}$$

where $\tilde{a}$ is the asymptotic level density parameter, δE_0 is the shell correction energy, and γ is the damping parameter. The asymptotic level density parameter is expressed as

$$\tilde{a}=\alpha_{\mathrm{V}}\mathcal{A}+\beta_{\mathrm{S}}\mathcal{A}^{2/3} \tag{11}$$

and the damping parameter is given by

$$\gamma=\gamma_0/\mathcal{A}^{1/3}. \tag{12}$$

The coefficients α_{V} and β_{S} correspond to the volume and surface components, respectively, which, along with γ_0 are taken to be phenomenological constants that are determined from a least-squares fit of the a parameters, and are given by (Belgya et al., 2006)

$$\alpha_{\mathrm{V}}=0.0959\pm0.0005\ \mathrm{MeV}^{-1} \tag{13}$$

$$\beta_{\mathrm{S}}=0.1468\pm0.0035\ \mathrm{MeV}^{-1} \tag{14}$$

$$\gamma_0=0.325\pm0.015\ \mathrm{MeV}^{-1}. \tag{15}$$

Future work will consider using the Monte Carlo intranuclear cascade model (MCMC), which includes multiple nucleon

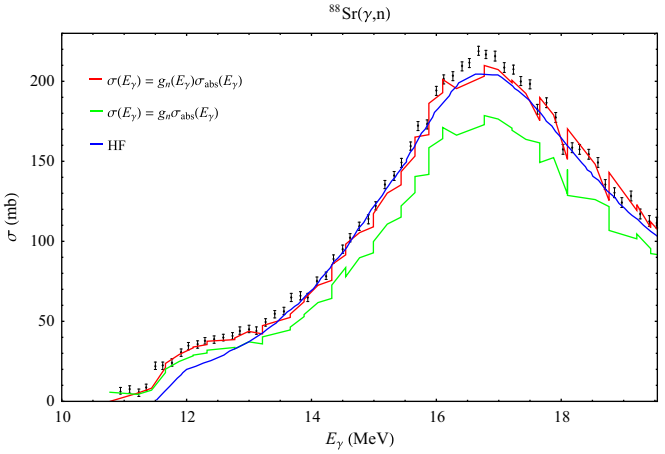

Fig. 1. Comparison of theoretical and experimental photoneutron cross section results for ^{88}Sr. The theoretical photoneutron cross sections are calculated using energy dependent WE (red) and energy independent (green) branching ratios. Experimental data (black) and theoretical HF data evaluated by KAERI (blue) are from IAEA (2000, p. 168). (For interpretation of the references to color in this figure caption, the reader is referred to the web version of this article.)

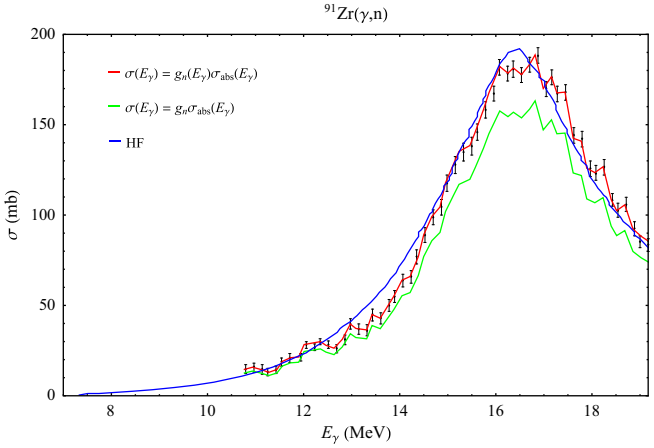

Fig. 2. Comparison of theoretical and experimental photoneutron cross section results for ^{91}Zr. The theoretical photoneutron cross sections are calculated using energy dependent WE (red) and energy independent (green) branching ratios. Experimental data (black) and theoretical HF data evaluated by CNDC (blue) are from IAEA (2000, p. 171). (For interpretation of the references to color in this figure caption, the reader is referred to the web version of this article.)

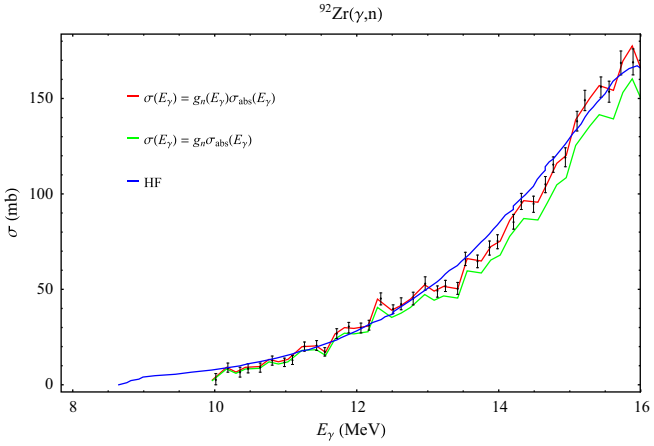

Fig. 3. Comparison of theoretical and experimental photoneutron cross section results for ^{92}Zr. The theoretical photoneutron cross sections are calculated using energy dependent WE (red) and energy independent (green) branching ratios. Experimental data (black) and theoretical HF data evaluated by CNDC (blue) are from IAEA (2000, p. 172). (For interpretation of the references to color in this figure caption, the reader is referred to the web version of this article.)

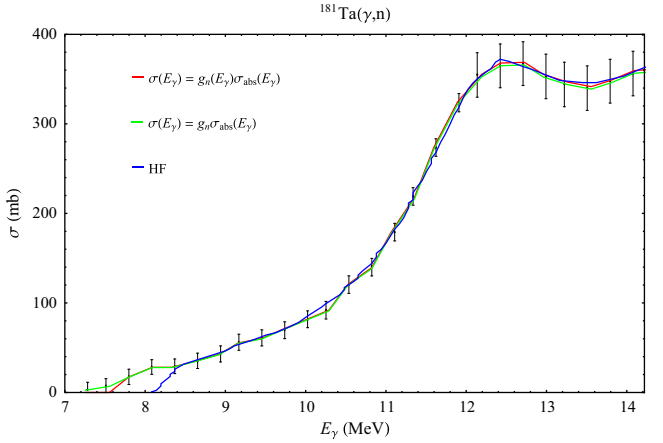

Fig. 4. Comparison of theoretical and experimental photoneutron cross section results for ^{181}Ta. The theoretical photoneutron cross sections are calculated using energy dependent WE (red) and energy independent (green) branching ratios. Experimental data (black) and theoretical WE data evaluated by JENDL (blue) are from IAEA (2000, p. 240). Theoretical photonuclear results obtained using energy dependent WE and energy independent branching ratios lie almost on top of each other. (For interpretation of the references to color in this figure caption, the reader is referred to the web version of this article.)

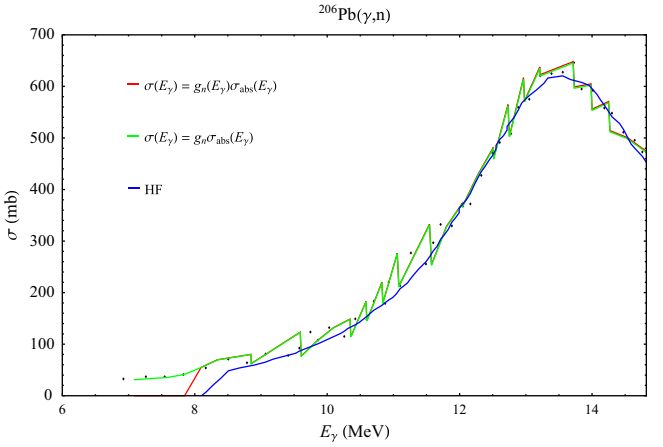

Fig. 5. Comparison of theoretical and experimental photoneutron cross section results for ^{206}Pb. The theoretical photoneutron cross sections are calculated using energy dependent WE (red) and energy independent (green) branching ratios. Experimental data (black) and theoretical HF data evaluated by LANL (blue) are from IAEA (2000, p. 249). Theoretical photonuclear results obtained using energy dependent WE and energy independent branching ratios lie almost on top of each other. (For interpretation of the references to color in this figure caption, the reader is referred to the web version of this article.)

emissions from the GDR decay and also pre-equilibrium emissions in the quasi-deuteron energy range. This model uses the WE statistical model successive times during the compound nucleus decay via a Monte Carlo evaporation/fission code.

4. Comparison to experiment

The photonuclear cross sections presented herein are calculated with Eq. (1) using the WE branching ratio given in Eq. (2) and experimental absorption cross sections, from reference (IAEA, 2000), for various photon energies up to the two neutron separation energy. Comparisons to experimental data and to theoretical HF predictions of the various groups discussed in Section 3.1 are made for a variety of target nuclei, as shown in Figs. 1–7.

It should be mentioned that the photonuclear results predicted with WE theory contain jumps. This behavior is anticipated. Experimental absorption cross section data were used to predict the WE results. Jumps in the plotted data will occur, because the photoparticle total cross section follows the shape of the absorption cross section. It is uncertain from the documentation and manuals for the GNASH and GUNF nuclear reaction codes (Chadwick and Young, 1995; IAEA, 2000; Lui and Zhang, 1998; Young et al., 1996) whether or not the HF predictions utilized an experimental or a parameterized photoabsorption cross section. The smooth predictions given by the HF method seem to indicate that a parameterized photoabsorption cross section may have been used. However, it is possible that a data smoothing technique was applied to eliminate jumps caused by using an experimental photoabsorption cross section. The oscillations in the WE calculations could be avoided if a Lorentzian GDR shape was applied, such as those investigated by Dietrich and Berman (1988). However, this work contains only comparisons to the actual data.

Also presented in this section are comparisons to photonuclear cross sections calculated from the product of experimental absorption cross sections from IAEA (2000) and energy independent

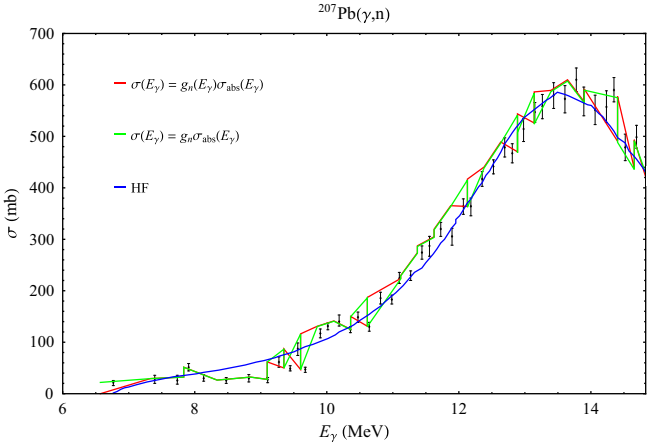

Fig. 6. Comparison of theoretical and experimental photoneutron cross section results for ^{207}Pb. The theoretical photoneutron cross sections are calculated using energy dependent WE (red) and energy independent (green) branching ratios. Experimental data (black) and theoretical HF data evaluated by LANL (blue) are from IAEA (2000, p. 250). Theoretical photonuclear results obtained using energy dependent WE and energy independent branching ratios lie almost on top of each other. (For interpretation of the references to color in this figure caption, the reader is referred to the web version of this article.)

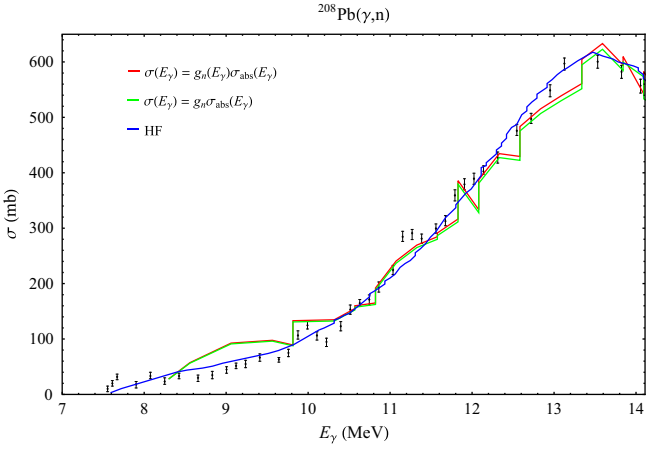

Fig. 7. Comparison of theoretical and experimental photoneutron cross section results for ^{208}Pb. The theoretical photoneutron cross sections are calculated using energy dependent WE (red) and energy independent (green) branching ratios. Experimental data (black) and theoretical HF data evaluated by LANL (blue) are from IAEA (2000, p. 251). Theoretical photonuclear results obtained using energy dependent WE and energy independent branching ratios lie almost on top of each other. (For interpretation of the references to color in this figure caption, the reader is referred to the web version of this article.)

branching ratios given in Eqs. (20) and (21) of Adamczyk and Norbury (2011). This analysis was initially introduced by Adamczyk and Norbury (2011), however, additional reactions are presented here. A better fit of the experimental data can be observed for the theoretical photonuclear cross sections calculated with energy dependent WE branching ratios, than those which applied energy independent branching ratios. However, the differences between the branching ratio methods decrease with increasing nuclei mass. The matching between the energy dependent and energy independent branching ratios is probably related with the small probability of charged particle emission due to the Coulomb barrier. This fact indicates that the reaction is largely dominated by single neutron emission, which in turn does not depend significantly on the proton energy below the two neutron separation energy.

5. Conclusion

Theoretical photonuclear cross sections, calculated with WE branching ratios, were compared to the HF predictions of various laboratories. Results indicate that WE theory and the HF method give comparable photonuclear cross sections for intermediate and heavy nuclei up the two neutron separation energy. The WE calculations presented neglect pre-equilibrium and multiple particle emissions; however, the WE and HF agreement provides qualitative confidence in the use of the WE theory as a reliable evaluation method for EMD cross section calculations in the region of applicability explored by Adamczyk and Norbury (2011). The WE branching ratio was also compared to an energy independent branching ratio for calculating photonuclear cross sections. Agreement between the two branching ratio methods was found for heavy nuclei, which indicates the dominance of single neutron emission.

References

Adamczyk, A., Norbury, J., 2011. Electromagnetic dissociation cross sections using Weisskopf–Ewing theory. Nucl. Technol. 175, 216–227.

Belgya, T., Bersillon, O., Noy, R.C., Fukahori, T., Zhigang, G., Goriely, S., Herman, M., Ignatyuk, A., Kailas, S., Koning, A., Oblozinsky, P., Plujko, V., Young, P., 2006. Handbook for Calculations of Nuclear Reaction Data. RIPL-2. Technical Report TECDOC-1506. IAEA. Vienna.

Bertulani, C., Baur, G., 1988. Electromagnetic processes in relativistic heavy ion collisions. Phys. Rep. 163, 299–408.

Bertulani, C., Danielewicz, P., 2004. Introduction to Nuclear Reactions. Institute of Physics Publishing, Bristol.

Brink, D., 1990. The compound nucleus at high excitation energy. Nucl. Phys. A 519, 3–16.

Brink, D. (Ed.), 2008. Workshop in Chaos and Collectivity in Many Body Systems, Dresden.

Chadwick, M., Young, P., 1995. Preequilibrium model for photonuclear reactions up to the pion threshold. Acta Phys. Slov. 45, 633–644.

Dietrich, S.S., Berman, B.L., 1988. Atlas of photoneutron cross sections obtained with monoenergetic photons. Atomic Data Nucl. Data Tables 38, 199–338.

Dostrovsky, I., Fraenkel, Z., Friedlander, G., 1959. Monte carlo calculations of nuclear evaporation processes. III. Applications to low-energy reactions. Phys. Rev. 116, 683–702.

Dostrovsky, I., Rabinowitz, P., Bivins, R., 1958. Monte Carlo calculations of high-energy nuclear interactions. I. Systematics of nuclear evaporation. Phys. Rev. 111, 1659–1676.

Frobrich, P., Lipperheide, R., 1996. Theory of Nuclear Reactions. Clarendon Press, Oxford.

Fukahori, T., 1991. No. JAERI-M 92-039. In: Proceedings of the Specialists' Meeting on High Energy Nuclear Data, Tokai.

Gadioli, E., Hodgson, P., 1992. Pre-Equilibrium Nuclear Reactions. Clarendon Press, Oxford.

Hodgson, P., 1987. Compound nucleus reactions. Rep. Prog. Phys. 50, 1171–1228.

Hussein, E., 2003. Handbook on Radiation Probing, Gauging, Imaging, and Analysis: Basics and Techniques, vol. I. Kluwer Academic, Norwell.

IAEA, 2000. Handbook on photonuclear data for applications—cross sections and spectra. TECDOC-Draft No. 3 edition.

Ignatyuk, A., Smirenkin, G., Tishin, A., 1975. Phenomenological description of the energy dependence of the level density parameter. Sov. J. Nucl. Phys. 21, 255–257.

Jackson, J., 1999. Classical Electrodynamics, third edition Wiley, New Jersey.

Lui, T., Zhang, J., 1998. Communication of Nuclear Data Progress No. 19. Beijing.

Norbury, J., Maung, K.M., 2007. Electromagnetic dissociation and space radiation. Acta Astronaut. 60, 770–774.

Norbury, J., Townsend, L., 1986. Electromagnetic Dissociation Effects in Galactic Heavy-Ion Fragmentation. Technical Report TP-2527. NASA.

Rodrigues, T.E., Martins, M.N., Garcia, C., Arruda-Neto, J.D.T., Mesa, J., Shtejer, K., Garcia, F., 2007. Photon-induced multiple particle emissions of ^{90}Zr and ^{nat}Zr from 10 to 140 MeV. Phys. Rev. C 75, 014605.

Talou, P., Kawano, T., Young, P., Chadwick, M., 2006. The McGNASH nuclear reaction code and its use for gas production cross-section calculations. Nucl. Instrum. Methods Phys. Res. Sect. A 562, 823–826.

Wilson, J., Shinn, J., Townsend, L., Tripathi, R., Badavi, F., Chun, S., 1994. NUCFRG2: A semiempirical nuclear fragmentation model. Nucl. Instrum. Methods Phys. Res. Sect. B 94, 95–102.

Wilson, J., Tripathi, R., Cucinotta, F., Shinn, J., Badavi, F., Chun, S., Norbury, J., Zeitlin, C., Heilbronn, L., Miller, J., 1995. NUCFRG2: An Evaluation of the Semiempirical Nuclear Fragmentation Database. Technical Report TP-3533. NASA.

Young, P., Arthur, E., Chadwick, M., 1996. Comprehensive Nuclear Model Calculations: Theory and Use of the GNASH code. In: Proceedings of the IAEA Workshop on Nuclear Reaction Data and Nuclear Reactors—Physics, Design, and Safety, Trieste.